Geophysical Research Letters

RESEARCH LETTER
10.1029/2018GL078287

Key Points:
- Whistler mode waves are excited at open field lines where magnetospheric and magnetosheath electrons mix and form an anisotropic distribution
- Whistler mode waves drive and modulate Langmuir waves as they propagate toward the X line
- Langmuir waves are excited by localized electron beams that are accelerated by whistlers via Landau resonance

Supporting Information:
- Supporting Information S1

Correspondence to:
J. Li,
jli@atmos.ucla.edu

Citation:
Li, J., Bortnik, J., An, X., Li, W., Russell, C. T., Zhou, M., et al. (2018). Local excitation of whistler mode waves and associated Langmuir waves at dayside reconnection regions. *Geophysical Research Letters*, *45*, 8793–8802. https://doi.org/10.1029/2018GL078287

Received 10 APR 2018
Accepted 22 AUG 2018
Accepted article online 27 AUG 2018
Published online 12 SEP 2018

Local Excitation of Whistler Mode Waves and Associated Langmuir Waves at Dayside Reconnection Regions

Jinxing Li[1], Jacob Bortnik[1], Xin An[1], Wen Li[2], Christopher T. Russell[3], Meng Zhou[4], Jean Berchem[4], Cong Zhao[3], Shan Wang[5], Roy B. Torbert[6], Olivier Le Contel[7], Robert E. Ergun[8], Per-Arne Lindqvist[9], Craig J. Pollock[10], and James L. Burch[11]

[1]Department of Atmospheric and Oceanic Sciences, University of California, Los Angeles, CA, USA, [2]Center for Space Physics, Boston University, Boston, MA, USA, [3]Earth Planetary and Space Sciences, University of California, Los Angeles, CA, USA, [4]Department of Physics and Astronomy, University of California, Los Angeles, CA, USA, [5]Astronomy Department, University of Maryland, College Park, MD, USA, [6]Institute for the Study of Earth, Oceans, and Space, University of New Hampshire, Durham, NH, USA, [7]Laboratoire de Physique des Plasmas, CNRS/Ecole Polytechnique/Sorbonne Université/Université Paris-Sud/Observatoire de Paris, Paris, France, [8]Laboratory of Atmospheric and Space Physics, University of Colorado Boulder, Boulder, CO, USA, [9]Department of Space and Plasma Physics, KTH Royal Institute of Technology, Stockholm, Sweden, [10]NASA, Goddard Space Flight Center, Greenbelt, MD, USA, [11]Southwest Research Institute, San Antonio, TX, USA

Abstract In the Earth's dayside reconnection boundary layer, whistler mode waves coincide with magnetic field openings and the formation of the resultant anisotropic electrons. Depending on the energy range of anisotropic electrons, whistlers can grow at frequencies in the upper and/or lower band. Observations show that whistler mode waves modulate Langmuir wave amplitude as they propagate toward the X line. Observations of whistler mode wave phase and Langmuir waves packets, as well as coincident electron measurements, reveal that whistler mode waves can accelerate electrons via Landau resonance at locations where $E_{||}$is antiparallel to the wave propagation direction. The accelerated electrons produce localized beams, which subsequently drive the periodically modulated Langmuir waves. The close association of those two wave modes reveals the microscale electron dynamics in the exhaust region, and the proposed mechanism could potentially be applied to explain the modulation events observed in planetary magnetospheres and in the solar wind.

Plain Language Summary The Sun's and Earth's magnetic field can merge and reconnect on dayside magnetopause. Using measurements from NASA's MMS spacecraft, we report that a class of electromagnetic wave, named whistler mode wave, coincides with the reconnected magnetic field lines. Besides, those whistlers are observed to modulate the electric field oscillations, known as Langmuir waves. Using high-resolution wave and particle measurements, we explain that the whistlers are locally excited when electrons from both sides of the magnetopause mix and form an unstable distribution. The modulated Langmuir waves are generated due to localized electron acceleration, which occurs when the velocity of electrons matches that of whistlers in the direction along the magnetic field. The whistler mode waves and associated Langmuir waves can be used as an additional tool to remotely sense the occurrence of magnetic reconnections.

1. Introduction

Dayside magnetic reconnection occurs when the Sun's and Earth's oppositely directed magnetic fields merge at the magnetopause. During this process, magnetic energy is explosively converted into kinetic and thermal energies of the plasma. Various plasma waves and structures at the electron scale have been suggested to be associated with dayside reconnection, including whistler mode waves, Langmuir waves, electrostatic solitary waves (ESW), electron cyclotron harmonic waves (ECH), electron acoustic waves, and double layers (e.g., Ergun, Holmes, S., et al., 2016; Ergun, Tucker, et al., 2016; Graham et al., 2016; Le Contel, Retinò, et al., 2016; Wilder et al., 2016; Zhou et al., 2016, 2018, and references therein). These waves may be capable of accelerating electrons, generating anomalous resistivity, and locally breaking the frozen-in condition in the electron and ion diffusion reconnection regions (Fujimoto et al., 2011).

Whistler mode waves have received much attention in reconnection studies. They have been suggested to facilitate the reconnection process (Deng & Matsumoto, 2001; Drake et al., 2008; Mandt et al., 1994), to

modulate the reconnection rate (Goldman et al., 2014), and to accelerate electrons near the magnetopause boundary (Jaynes et al., 2016; Sharma et al., 2017). In addition, the standing oblique electrostatic whistler waves near the electron diffusion region edge may cause local dissipation (Burch, Ergun, et al., 2018). However, the origin of whistler mode waves and how they lead to energy transfer and dissipation in the reconnection region are still not well understood. Understanding the microscopic interactions between the waves and particles in reconnection regions requires high-resolution measurements both in the temporal and spatial domain. The Magnetospheric Multiscale (MMS) mission (Burch et al., 2016) consists of four identical satellites with small separations, providing an unprecedented opportunity to measure the microscale dynamics of particles and waves.

At dayside reconnection regions, whistler mode waves are often accompanied by higher-frequency electrostatic waves, which may potentially provide important information on resolving the nature of the rapid and microscale nonlinear interactions that cannot be directly measured through low-cadence plasma data. ESW have been observed to be associated with whistler mode waves in the electron diffusion region (Tang et al., 2013). Wilder et al. (2016, 2017) reported two reconnection events in which electrostatic bipolar solitons were in phase with whistler mode waves, while Langmuir waves were also observed. Recently, Burch, Webster, et al. (2018) reported the coexistence of whistler mode wave and beam mode waves in the electron diffusion region. How the whistler mode and electrostatic mode waves are coupled and whether the coupling of these wave modes can assist in sensing the highly dynamic particle evolution in the reconnection regions are of great general interest to reconnection studies.

In this paper, we use the high-resolution MMS measurements at the dayside magnetopause to report that whistler mode waves excited in the boundary layer can drive and modulate electrostatic Langmuir wave bursts as they propagate toward the reconnection diffusion region. We explain the occurrence of such a nonlinear process by examining the phase and amplitude of the two wave modes and high temporal resolution electron measurements. The correlation between modulated Langmuir waves, the harmonic structure, and the rising-tone feature of whistlers is also discussed.

2. Data Set

The present study uses measurements of electric and magnetic fields, waves, and particles from the comprehensive suites of instruments onboard the MMS spacecraft (Burch et al., 2016). The FIELDS suite provides measurements of 3-D magnetic and electric waves (Torbert et al., 2016). The magnetic field measured by the fluxgate magnetometer (FGM, 128 samples/s in burst mode; Russell et al., 2016) is used to study the magnetic field topology. The search coil magnetometer (SCM) provides burst mode magnetic waveform measurements (8,192 samples/s; Le Contel, Leroy, et al., 2016). The spin-plane double-probes (SDP; Lindqvist et al., 2016) and the axial double probes (ADP; Ergun, Tucker, et al., 2016) provide electric waveform data at two rates: 8,192 samples/s (direct current E, DCE) and 65,536 samples/s (half maximum frequency E, HMFE), enabling us to identify a variety of high-frequency electromagnetic and electrostatic waves. The Fast Plasma Investigator (FPI; Pollock et al., 2016) provides 3-D directional electron and ion flux measurements over an energy range from 10 eV to 30 keV, with unprecedented temporal resolution (30 ms for electrons and 150 ms for ions).

3. Event Overview and Wave Observations

Figure 1 shows an overview of MMS-4 data on 1 October 2015 near a dayside reconnection site at $r_{GSM} = (4.5, 9.2, -4.4)\ R_E$. Figure 1a shows the magnetic field measurements in **lmn** coordinates. Here **n** is normal to the magnetopause boundary and away from Earth (calculated as $\mathbf{b}_{sheath} \times \mathbf{b}_{sphere}$), **m** is in the direction of $\mathbf{n} \times (\mathbf{B}_{sphere} - \mathbf{B}_{sheath})$, and $\mathbf{l} = \mathbf{m} \times \mathbf{n}$ completes the boundary normal coordinates and is roughly in the direction of the magnetic field on the magnetosphere side, as illustrated in Figure 2. At 17:21:36 UT the magnetic field B_l component reversed (Figure 1a), indicating a crossing of the magnetopause. The ion flow was antiparallel to the **l** direction (Figure 1d), suggesting that the spacecraft was southward of the X line. The spacecraft was initially in the magnetosheath boundary layer characterized by high-density cold plasmas (Figures 1b and 1c), and then traveled through the low-latitude boundary layer (LLBL) between 17:21:36 and 17:21:46 UT, identified by the counterstreaming cold electron flow from the magnetosheath and hot electron flow from the magnetosphere (Figures 1g and 1i), and the observation of a D-shaped ion velocity distribution (Figure S1 in the supporting information; e.g., Broll et al., 2017; Fuselier et al., 2017). At 17:21:46 UT, the satellite encountered the closed

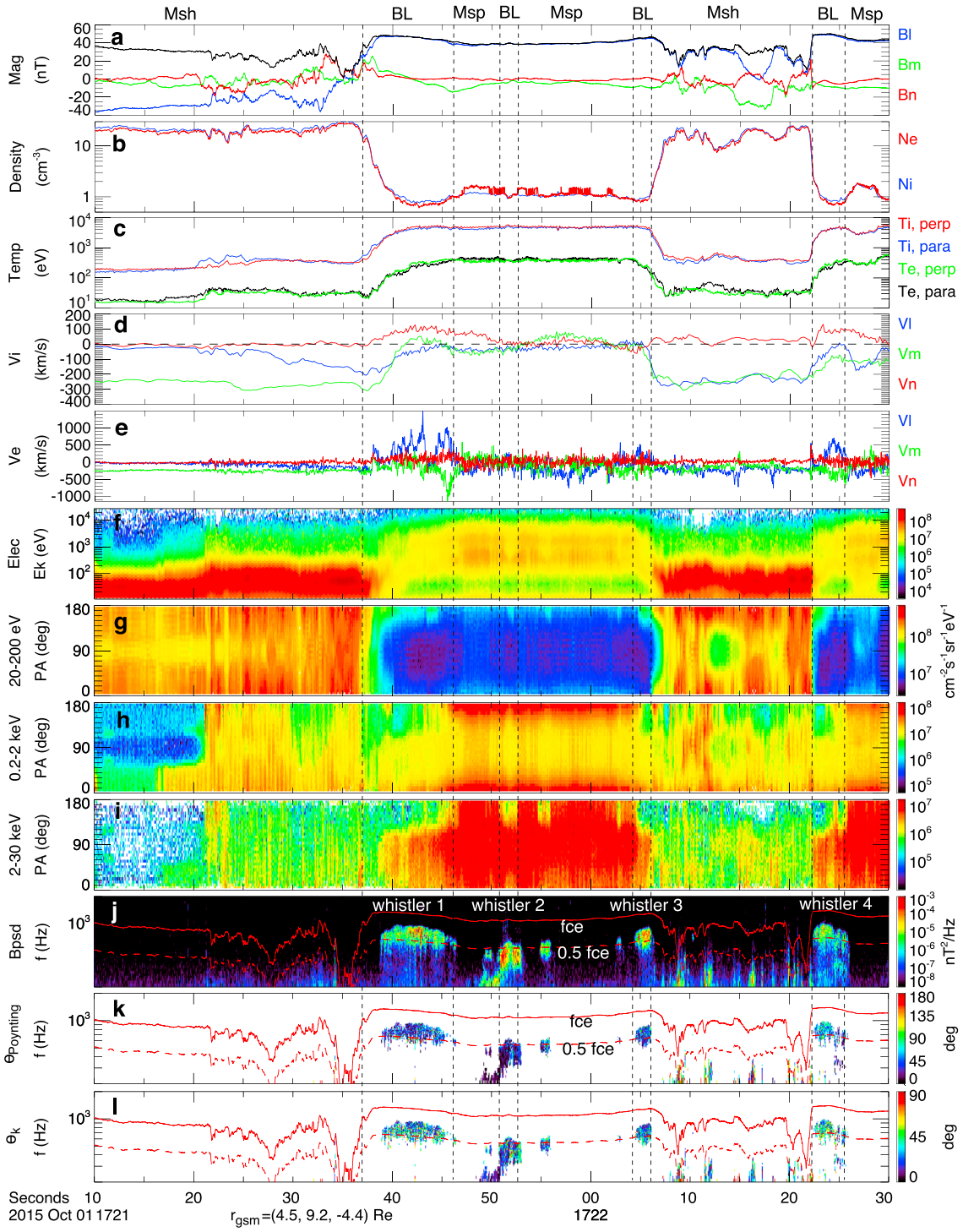

Figure 1. Overview of MMS-4 burst mode measurements in a magnetopause crossing event. (a) Magnetic field in **lmn** coordinates; (b) electron and ion densities, (c) electron and ion temperature; (d) ion and (e) electron bulk velocities in **lmn** coordinates, and (f) electron omnidirectional flux. (g–i) Electron pitch angle distributions over the energy range of 20–200 eV, 0.2–2 keV, and 2–30 keV, respectively. (j) Magnetic power spectral density measured at a cadence of 8,192 samples per second. (k) The angle between the wave Poynting flux and the magnetic field. (l) The angle between the ***k*** vector and the magnetic field. MMS = Magnetospheric Multiscale.

field lines of the magnetosphere, as indicated by the symmetric hot electron pitch angle distribution. The spacecraft traveled back and forth across the boundary several times. The possible trajectory of the spacecraft with respect to the magnetic field configuration is sketched in Figure 2.

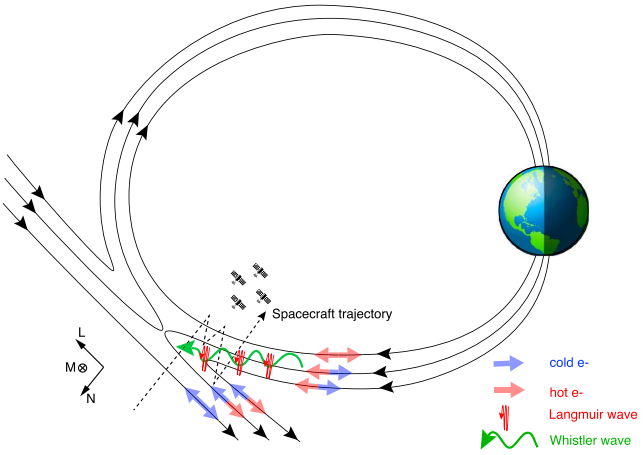

Figure 2. Schematic illustration of magnetic field topology, as well as wave and electron dynamics. At open field lines of the boundary layers, the cold magnetosheath electrons mix with the hot magnetospheric electrons. The whistler mode waves propagate toward the X line, and modulate Langmuir wave burst at locations of negative $E_{||}$. The possible spacecraft trajectory with respect to the moving boundary is illustrated with a black dashed line.

Figure 1j shows the burst mode magnetic power spectral density (*B*psd) measured by SCM. A whistler mode wave (hereafter, Whistler-1) was observed in the upper band ($0.5\ f_{ce} < f < f_{ce}$, where f_{ce} represents electron gyrofrequency) when the spacecraft traveled into the boundary layer for the first time. Between 17:21:51 and 17:21:53 UT, a second whistler mode wave (hereafter, Whistler-2) was detected in the lower band ($f < 0.5\ f_{ce}$). A few more upper-band whistler mode waves were observed later, whose onset coincided well with the opening of magnetic field identified from electron flows. The Poynting flux of those whistler mode waves was roughly parallel to the magnetic field toward the direction of the X line (Figure 1k). The wave normal angles (Figure 1l), calculated using the Means (1972) method, indicate that the upper-band whistler mode waves are in general more oblique than the lower-band waves. Direct observation also shows that the upper-band whistlers generally have a significantly larger parallel electric field compared to the lower-band waves.

Electrostatic bursts were also observed in association with whistler mode waves during the crossing of the LLBLs. Figure 3a shows magnetic waveforms in field-aligned coordinates measured during a short period of Whistler-1. We transformed the original waveform to the field-aligned coordinate system based on the magnetic field in the geocentric solar ecliptic (GSE) coordinates, and no band-pass filtering was applied. The HMFE electric waveform, shown in Figure 3b, exhibits periodic bursts in the $E_{||}$component. Those electrostatic bursts are identified as Langmuir waves because they oscillate in the direction parallel to the magnetic field and their frequencies were around the electron plasma frequency, f_{pe} (Figure 3c). Although the electric field amplitude of Langmuir waves greatly exceeds that of the whistler mode waves, we note that the majority of whistler mode wave energy is stored in the magnetic component, and the overall energy density of whistler mode waves ($\tilde{B}_w^2/2\mu_0 = 8.9\times10^{-15}\ \mathrm{N/m^2}$) significantly exceeds the peak energy density of electrostatic Langmuir waves ($\epsilon_0 E_w^2/2 = 1.8\times10^{-15}\ \mathrm{N/m^2}$). As those two large-amplitude wave modes propagate toward X line, they may potentially contribute to the overall electron acceleration and energy dissipation processes.

The Langmuir wave bursts are seen to be modulated by the whistler mode waves and are generally excited near the whistler mode $E_{||}$ minima (black line in Figure 3c, DCE waveform). These bursts are similar to the Langmuir waves modulated by whistler mode chorus waves in the radiation belts, which were recently reported by Li et al. (2017). The inner magnetospheric Langmuir bursts observed in the radiation belts were generally excited at $E_{||}$ minima (maxima) when whistler mode waves propagate roughly parallel (antiparallel) to the magnetic field. The whistler mode wave phase in which Langmuir waves are excited in the present study is thus consistent with that observed in the radiation belts. At time of the lower-band Whistler-2, electrostatic Langmuir bursts were also periodically observed near whistler mode $E_{||}$minima (Figures 3d–3f). At time of Whistler-3 (17:22:04–17:22:06 UT), HMFE waveform measured from all four spacecraft simultaneously detected Langmuir bursts at locations generally near the $E_{||}$minima of the whistler mode waves (Figures 3g–3n), though the measurements suggest that the whistler mode waves were not coherent at the present interspacecraft distance (~30 km).

4. Particle Measurements and Instability Analysis

Two mechanisms have been suggested for the generation of whistler mode waves: cyclotron resonance with anisotropic electrons, in which the Doppler-shifted wave frequency matches the electron cyclotron frequency, $\omega - k_{||}v_{||} = \Omega_{ce}$, and Landau resonance with electron beams, in which the parallel wave phase velocity matches the beam velocity, $\omega/k_{||} = v_{||}$ (Kennel & Petschek, 1966; Li et al., 2010; Mourenas et al., 2015; Wilder et al., 2017). Figure 4a shows 90-ms-averaged electron phase space density (PSD) distributions in the parallel (averaged within 0–30°and 150–180° pitch angles) and perpendicular (averaged within 85–95° pitch angles) directions measured at the time of Whistler-1. Using the wave and background plasma parameters from observations ($B_0 = 46$ nT, $N_e = 1.0\ \mathrm{cm^{-3}}$, $f = 0.54$–$0.62\ f_{ce}$, where f_{ce} represents the electron gyrofrequency, wave normal angle θ_k = 20–40°) and assuming the cold plasma dispersion relation of whistler

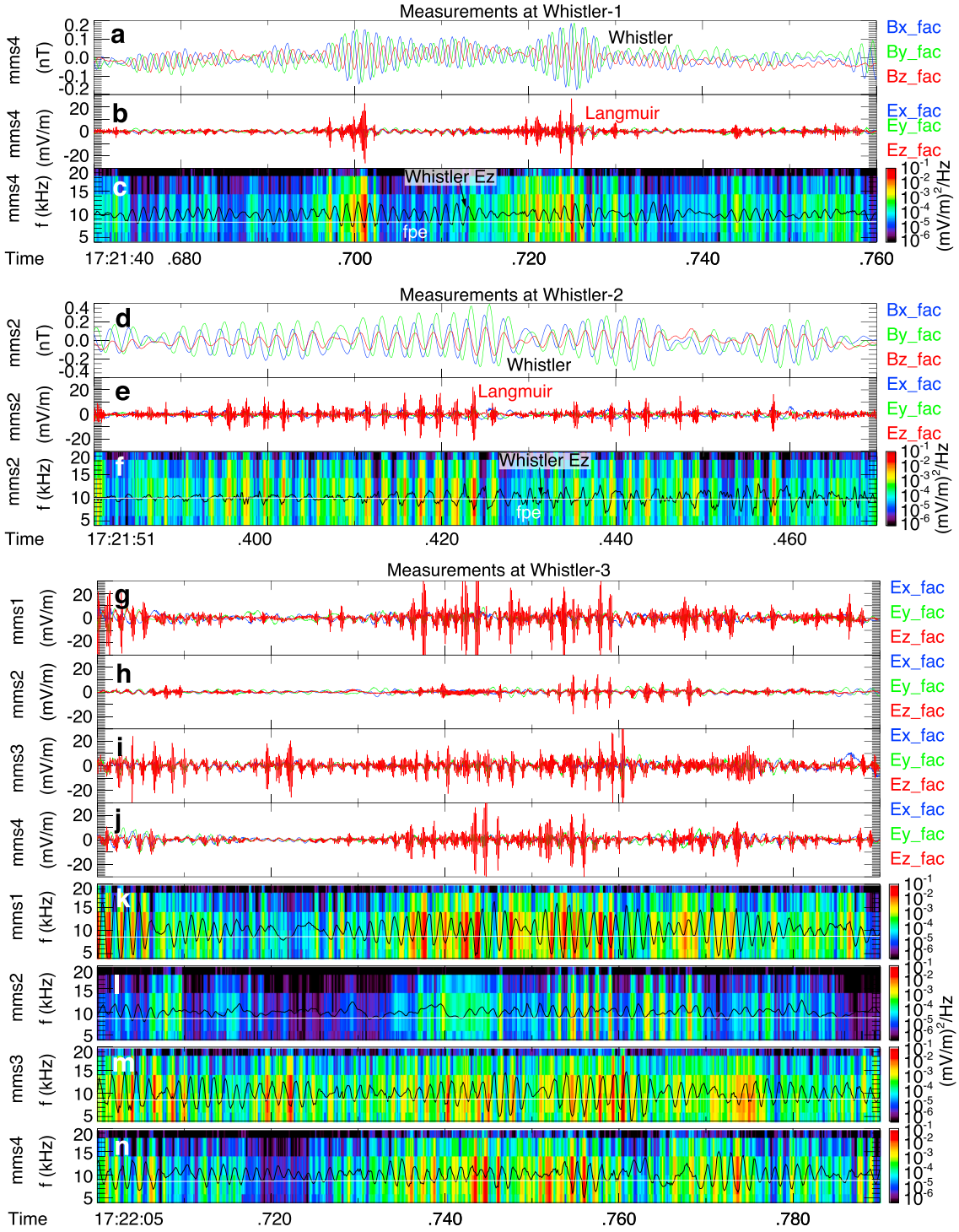

Figure 3. (a) The magnetic waveform, and (b) the HMFE electric waveform measured during a 90-ms period at Whistler-1. (c) tThe electric power spectral density by Fourier transformation overplotted with f_{pe} (white line) and amplified Ez (DCE waveform, black line). (d–f) The wave measurements at Whistler-2. (g–j) The electric waveform measurements by four satellites, respectively, at Whistler-3, and (k–n) the electric spectra. Most Langmuir waves were excited near Ez minima of whistler mode waves.

mode waves (Stix, 1962), the calculated cyclotron resonant velocity range is $v_{||}$~ −10,000 to −18,000 km/s. The electron distribution shows an anisotropy ($T_{anti\text{-}||} < T_{\perp}$) at this velocity range, which is due to the magnetic field opening and lack of hot field-aligned electrons from the sheath. The Landau resonant

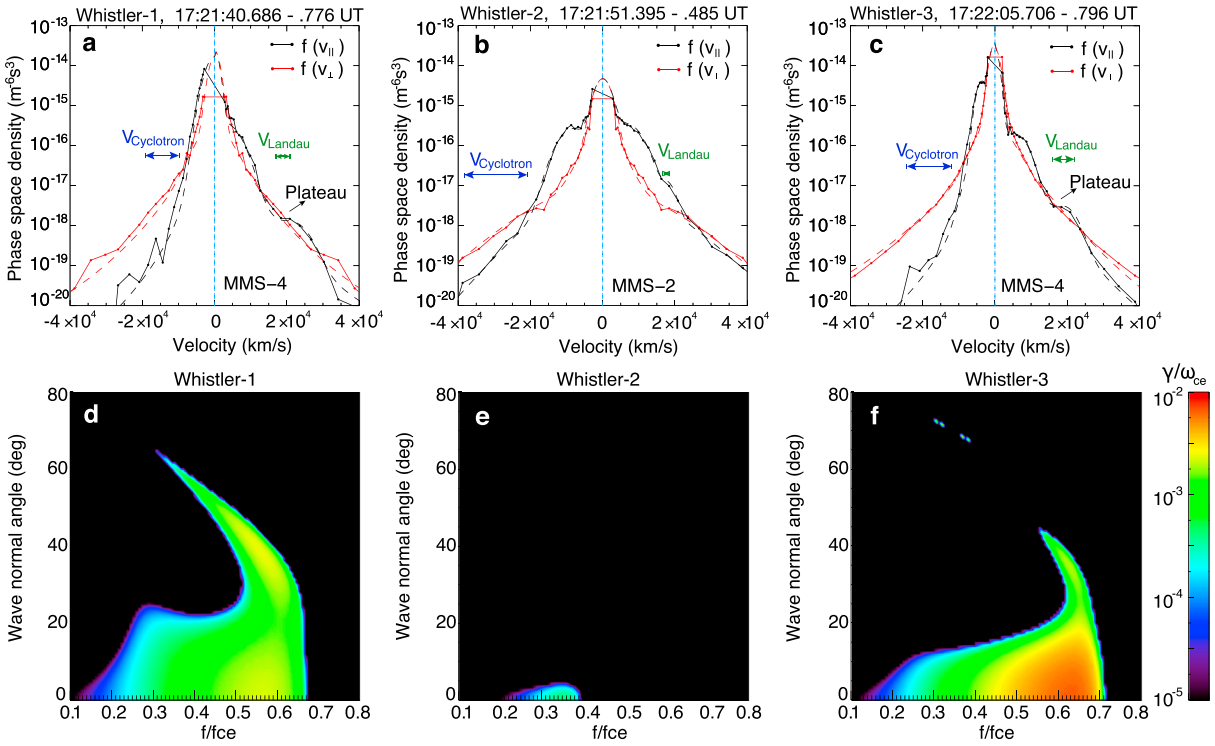

Figure 4. (a–c) The burst mode electron phase space density in parallel and perpendicular directions measured during a short period of Whistler 1, 2, and 3, respectively. The solid lines represent the measured data and the dashed lines represent the fitted distributions. (d–f) The linear growth rate of whistler mode waves as a function of frequency and wave normal angle for each case, calculated as the summation of growth/damping rates caused by cyclotron resonance and Landau resonance.

velocity range of Whistler-1 is from ~17,000 to ~21,000 km/s, where an electron PSD plateau is clearly observed.

To quantitatively evaluate the growth rate of the upper-band wave Whistler-1, we first model the observed electron PSD as a summation of bi-Maxwellian distributions and kappa distributions (see supporting information), and the modeled PSD profiles are illustrated as dashed lines in Figure 4a. The linear growth rates (Kennel & Petschek, 1966) of whistler mode waves are calculated as the total of the contributions from cyclotron resonance and Landau resonance. The total linear growth rates versus frequency and wave normal angle, shown in Figure 4d, indicate that the whistler mode waves predominantly grow in the upper band in a wave normal angle range of 0–40°. The growth rates of lower-band whistlers are significantly lower, and the flux of high-energy electrons that drive lower-band waves is also low, thus the saturation amplitudes of lower-band waves is expected to be much lower than those of upper-band whistlers, roughly consistent with observations. The growth timescale $1/\gamma$ of the upper-band whistlers is ~0.1 s, which is longer than the time resolution of the electron measurements (30 ms), and therefore, the anisotropic electron distribution should be observable by the MMS spacecraft before wave saturation. The electron PSD at the time of Whistler-3 (Figure 4c) is similar to those at time of Whistler-1, and the linear growth rate scenario (Figure 4f) shows an excellent agreement with the wave observations.

Figure 4b displays the electron PSD measured at the second boundary layer crossing where lower band Whistler-2 was detected. The electron anisotropy was observed at larger velocities: $v_{||} < -22{,}000$ km/s. This energy range coincides with the calculated cyclotron resonant velocity of lower-band whistlers, which is from ~ −21,000 to −38,000 km/s ($f = 0.32$–$0.46\ f_{ce}$, $\theta_k = 5$–$30°$, $B_0 = 39$ nT, $N_e = 1\ \mathrm{cm}^{-3}$). The linear growth calculation, shown in Figure 4e, indicates that whistler mode waves can be excited only in the lower band and at small wave normal angles. This explains the lower-band whistlers with very small wave normal angles observed at this boundary crossing. The upper-band whistler mode waves cannot be excited because of the negative anisotropy at resonant energies ($T_{\text{anti-}||} > T_\perp$). Oblique lower-band whistler mode waves cannot be generated, either, due to dominant Landau damping effects (not shown).

Based on our understanding of quasilinear theory, the whistler mode waves should flatten the electron PSD near the Landau resonant velocity via Landau resonant acceleration after several wave periods. However, linear theory alone is not adequate to explain the periodic excitation of Langmuir wave bursts. Based on a nonlinear interaction perspective, the electrostatic potential of whistler mode waves can trap the Landau resonant electrons, which can be accelerated at wave phases where $E_{||}$is opposite to the resonant velocity $v_{||}$(thus, the kinetic energy variation $\Delta E_k \propto qv_{||}E_{||}$is positive; Agapitov et al., 2015; Artemyev et al., 2013; Nunn & Omura, 2015; Shklyar & Matsumoto, 2009). In the present study, the resonant velocity $v_{||}$, which equals the parallel phase velocity of whistlers, is positive; hence, the trapped electrons are accelerated at locations with negative $E_{||}$. The accelerated electrons form localized beams which instantaneously excite Langmuir waves to relax the localized weak beam instability. This mechanism explains the periodic excitation of Langmuir waves observed near whistler mode $E_{||}$minima. The large amplitude Langmuir waves (~30 mV/m) smooth out the localized electron beams and cause acceleration at energies slightly higher than the Landau trapping energy.

The electron beam was not captured at the time of Whistler-2, possibly because the $E_{||}$amplitude of the quasiparallel Whistler-2 is much smaller than that of the upper-band oblique Whistler-1 and Whistler-3; hence, the Landau resonance is less pronounced. In addition, the estimated Landau resonant velocity range of Whistler-2 is too narrow (~17,000–18,100 km/s), and the electron beam, even if it existed, cannot be captured due to limited energy resolution of the FPI instrument. For all those cases, the localized electron beam energy density is hard to estimate due to limited spatial and temporal resolution of particle measurements compared to the beam scale. Since the waves act as a medium to transfer energy in the Landau trapping (Shklyar, 2011), the energy density of the whistlers and the beams are incomparable.

5. Discussion

The close correlation between whistler mode waves and Langmuir waves presented above is not rare or unique and was detected in a number of reported reconnection events. Wilder et al. (2016) reported the 19 September 2015 reconnection event in which nonlinear ESW and Langmuir waves were observed in association with whistler mode waves. Here we report that those Langmuir waves were also driven and modulated by whistler mode waves (see Figure S2 and S3 in the supporting information). The anisotropic electrons observed over the cyclotron resonant energy of whistlers and an electron beam near Landau resonant velocity (Figure S4 in the supporting information) are consistent with the nonlinear mechanism proposed above. Most recently, Burch, Webster, et al. (2018) reported a whistler mode wave and electrostatic beam mode wave near a reconnection diffusion region southward of the X line on 23 November 2016. We show that those electrostatic beam mode waves were modulated by whistler mode waves (Figure S4 in the supporting information). However, in this case, a beam with a velocity smaller than electron thermal velocity was observed, and the dispersion relation of the beam mode waves is different from the Langmuir waves generated from bump-on-tail instability because Landau damping cannot be neglected in the dispersion relation (Reinleitner et al., 1983).

In the radiation belts, the lower-band whistler mode chorus waves that drive and modulate Langmuir waves exhibit two nonlinear features in the spectra, the multiband and rising-tone structures (Li et al., 2017). In the present study, the lower-band whistler mode waves do not exhibit a rising-tone structure, and it is hard to determine the existence of harmonics because those whistlers are broadband and structureless. However, the upper-band whistler mode waves observed at time of Whistler-1 exhibited a clear discrete rising-tone structure in the magnetic power spectral density, as shown in Figure 5a. The electric power spectral densities, shown in Figure 5b, present harmonics of those rising-tone emissions, especially the high-intensity ones, as well as coincident Langmuir waves. The generation of chorus waves with rising-tones and harmonic structures in the radiation belts, although having been investigated in a few previous studies (e.g., Kellogg et al., 2010; Li et al., 2011; Omura & Summers, 2006), still remains as an open question. Since those nonlinear features also exist in the dayside reconnection region, the electron measurements from MMS spacecraft with an unprecedented high cadence (~750 times higher than that from Van Allen Probes) may provide an alternative data source to study the underlying mechanisms. Whistler mode waves in space plasmas may also be associated with other nonlinear processes, such as phase trapping and bunching (Bortnik et al., 2008), and electrostatic steepening (Agapitov et al., 2018). The coincident electrostatic waves at higher frequencies may potentially assist us in revealing those nonlinear processes.

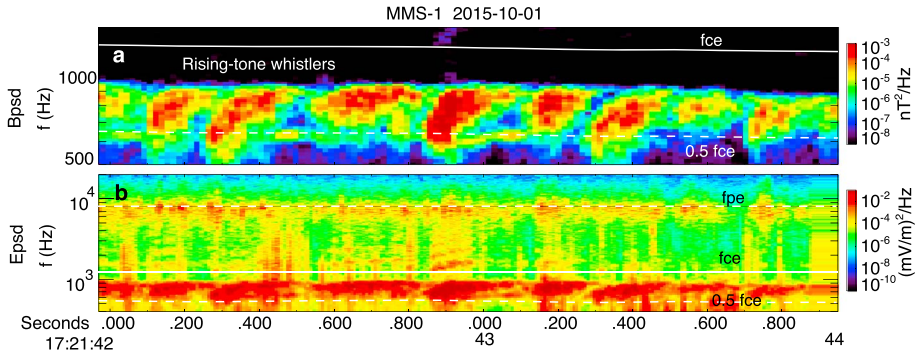

Figure 5. (a) Wave magnetic power spectral densities measured at time of Whistler-1 by MMS-1, showing discrete rising-tone upper band whistler modes emissions. (2) Wave electric power spectral densities measurements, showing evident harmonics of whistler mode waves and coincident Langmuir waves. MMS = Magnetospheric Multiscale.

The proposed mechanism for interactions between whistler and Langmuir modes and electrons has a number of implications for a wide range of space plasma environments. Whistler mode wave modulation of Langmuir waves was first observed in Earth's outer magnetosphere by ISEE-1 (Reinleitner et al., 1982). Voyager-1 and Voyager-2 detected numerous episodes of Langmuir waves modulated by whistler mode waves in Jovian middle magnetosphere both on the dayside and nightside (Reinleitner et al., 1984). A similar modulation event was also observed at Saturn's magnetosphere (Kurth et al., 1983). These two wave modes had also been observed to be coherently correlated in the solar wind both at L1 point by ISEE-3 (Kennel et al., 1980) and at 3.6 A.U. by Ulysses (Kellog et al., 1992). The proposed microscopic interaction mechanism may also have implications for a laboratory plasma environment where those two wave modes were observed to coexist (An et al., 2016, 2017).

6. Conclusions

In this paper, we showed that the onset of whistler mode waves and electrostatic Langmuir waves coincide with the crossing of boundary layers near the dayside reconnection region. Both upper-band and lower-band whistler mode waves can drive and modulate Langmuir wave bursts. In the magnetopause boundary layer, the parallel component of the hot magnetospheric electrons streams toward the X line and seldom comes back, while the perpendicular component remains intact, thus an anisotropic distribution is formed. Depending on the energy range of anisotropic electrons, whistler mode waves may be excited in the upper band or/and lower band frequency ranges. The electrons in Landau resonance with the whistler mode waves can be trapped in the wave field and are accelerated at locations where the parallel electric field $E_{||}$is opposite to the direction of resonant velocity $v_{||}$. The accelerated electrons in the trapped zone produce electron beams, which instantaneously excite periodically modulated Langmuir waves due to a weak beam instability. Since the onset of the whistler mode waves and electrostatic Langmuir waves marks the opening of magnetic field lines, the association between these waves could be used as an additional tool to remotely sense the occurrence of reconnection. The modulation between whistler mode waves and electrostatic Langmuir waves can reveal important information on the nonlinear interaction process that occurs not only in the Earth's reconnection regions but also in planetary magnetosphere and in the solar wind.

Acknowledgments
J. L. and J. Bortnik would like to acknowledge grant DE-SC0010578 from the U.S. Department of Energy and the National Science Foundation through the NSF/DOE Partnership in Basic Plasma Science and Engineering; and grants NNX16AG21G and NNX14AN85G from NASA. W. L. would like to acknowledge the NASA grant NNX17AD15G, AFOSR grant FA9550-15-1-0158, NSF grant AGS-1723342, and the Alfred P. Sloan Research Fellowship FG-2018-10936. The French involvement (SCM) on MMS is supported by CNES and CNRS. The entire MMS data are publically available online at https://lasp.colorado.edu/mms/sdc/public/links/. All of the data plots in this paper were generated with SPEDAS software (http://spedas.org/).

References

Agapitov, O., Drake, J. F., Vasko, I., Mozer, F. S., Artemyev, A., Krasnoselskikh, V., et al. (2018). Nonlinear electrostatic steepening of whistler waves: The guiding factors and dynamics in inhomogeneous systems. *Geophysical Research Letters*, *45*, 2168–2176. https://doi.org/10.1002/2017GL076957

Agapitov, O. V., Artemyev, A. V., Mourenas, D., Mozer, F. S., & Krasnoselskikh, V. (2015). Nonlinear local parallel acceleration of electrons through landau trapping by oblique whistler mode waves in the outer radiation belt. *Geophysical Research Letters*, *42*, 10,140–10,149. https://doi.org/10.1002/2015GL066887

An, X., Bortnik, J., van Compernolle, B., Decyk, V., & Thorne, R. (2017). Electrostatic and whistler instabilities excited by an electron beam. *Physics of Plasmas*, *24*(7), 072116. https://doi.org/10.1063/1.4986511

An, X., van Compernolle, B., Bortnik, J., Thorne, R. M., Chen, L., & Li, W. (2016). Resonant excitation of whistler waves by a helical electron beam. *Geophysical Research Letters*, *43*, 2413–2421. https://doi.org/10.1002/2015GL067126

Artemyev, A. V., Vasiliev, A. A., Mourenas, D., Agapitov, O. V., & Krasnoselskikh, V. V. (2013). Nonlinear electron acceleration by oblique whistler waves: Landau resonance vs. cyclotron resonance. *Physics of Plasmas*, *20*(12), 122901. https://doi.org/10.1063/1.4836595

Bortnik, J., Thorne, R. M., & Inan, U. S. (2008). Nonlinear interaction of energetic electrons with large amplitude chorus. *Geophysical Research Letters*, *35*, L21102. https://doi.org/10.1029/2008GL035500

Broll, J. M., Fuselier, S. A., & Trattner, K. J. (2017). Locating dayside magnetopause reconnection with exhaust ion distributions. *Journal of Geophysical Research: Space Physics*, *122*, 5105–5113. https://doi.org/10.1002/2016JA023590

Burch, J. L., Ergun, R. E., Cassak, P. A., Webster, J. M., Torbert, R. B., Giles, B. L., et al. (2018). Localized oscillatory energy conversion in magnetopause reconnection. *Geophysical Research Letters*, *45*, 1237–1245. https://doi.org/10.1002/2017GL076809

Burch, J. L., Moore, T. E., Torbert, R. B., & Giles, B. L. (2016). Magnetospheric multiscale overview and science objectives. *Space Science Reviews*, *199*(1-4), 5–21. https://doi.org/10.1007/s11214-015-0164-9

Burch, J. L., Webster, J. M., Genestreti, K. J., Torbert, R. B., Giles, B. L., Fuselier, S. A., et al. (2018). Wave phenomena and beam-plasma interactions at the magnetopause reconnection region. *Journal of Geophysical Research: Space Physics*, *123*, 1118–1133. https://doi.org/10.1002/2017JA024789

Deng, X. H., & Matsumoto, H. (2001). Rapid magnetic reconnection in the Earth's magnetosphere mediated by whistler waves. *Nature*, *410*(6828), 557–560. https://doi.org/10.1038/35069018

Drake, J. F., Shay, M. a., & Swisdak, M. (2008). The hall fields and fast magnetic reconnection. *Physics of Plasmas*, *15*(4), 042306. https://doi.org/10.1063/1.2901194

Ergun, R. E., Holmes, J. C., Goodrich, K. A., Wilder, F. D., Stawarz, J. E., Eriksson, S., et al. (2016). Magnetospheric multiscale observations of large-amplitude, parallel, electrostatic waves associated with magnetic reconnection at the magnetopause. *Geophysical Research Letters*, *43*, 5626–5634. https://doi.org/10.1002/2016GL068992

Ergun, R. E., Tucker, S., Westfall, J., Goodrich, K. A., Malaspina, D. M., Summers, D., et al. (2016). The axial double probe and fields signal processing for the MMS mission. *Space Science Reviews*, *199*, 167–188. https://doi.org/10.1007/s11214-014-0115-x

Fujimoto, M., Shinohara, I., & Kojima, H. (2011). Reconnection and waves: A review with a perspective. *Space Science Reviews*, *160*(1-4), 123–143. https://doi.org/10.1007/s11214-011-9807-7

Fuselier, S. A., Vines, S. K., Burch, J. L., Petrinec, S. M., Trattner, K. J., Cassak, P. A., et al. (2017). Large-scale characteristics of reconnection diffusion regions and associated magnetopause crossings observed by MMS. *Journal of Geophysical Research: Space Physics*, *122*, 5466–5486. https://doi.org/10.1002/2017JA024024

Goldman, M. V., Newman, D. L., Lapenta, G., Andersson, L., Gosling, J. T., Eriksson, S., et al. (2014). Cerenkov emission of quasiparallel whistlers by fast electron phase-space holes during magnetic reconnection. *Physical Review Letters*, *112*(14), 145002. https://doi.org/10.1103/PhysRevLett.112.145002

Graham, D. B., Khotyaintsev, Y. V., Vaivads, A., & André, M. (2016). Electrostatic solitary waves and electrostatic waves at the magnetopause. *Journal of Geophysical Research: Space Physics*, *121*, 3069–3092. https://doi.org/10.1002/2015JA021527

Jaynes, A. N., Turner, D. L., Wilder, F. D., Osmane, A., Baker, D. N., Blake, J. B., et al. (2016). Energetic electron acceleration observed by MMS in the vicinity of an X-line crossing. *Geophysical Research Letters*, *43*, 7356–7363. https://doi.org/10.1002/2016GL069206

Kellog, P. J., Goetz, K., Lin, N., Monson, S. J., Balogh, A., & Forsyth, R. J. (1992). Low frequency magnetic signals associated with Langmuir waves. *Geophysical Research Letters*, *19*(12), 1299–1302. https://doi.org/10.1029/92GL01033

Kellogg, P. J., Cattell, C. A., Goetz, K., Monson, S. J., & Wilson, L. B. III (2010). Electron trapping and charge transport by large amplitude whistlers. *Geophysical Research Letters*, *37*, L20106. https://doi.org/10.1029/2010GL044845

Kennel, C. F., & Petschek, H. E. (1966). Limit on stable trapped particle fluxes. *Journal of Geophysical Research*, *71*(1), 1–28. https://doi.org/10.1029/JZ071i001p00001

Kennel, C. F., Scarf, F. L., Coroniti, F. V., Fredricks, R. W., Gurnett, D. A., & Smith, E. J. (1980). Correlated whistler and electron plasma oscillation bursts detected on ISEE-3. *Geophysical Research Letters*, *7*(2), 129–132. https://doi.org/10.1029/GL007i002p00129

Kurth, W. S., Scarf, F. L., Gurnett, D. A., & Barbosa, D. D. (1983). A survey of electrostatic waves in Saturn's magnetosphere. *Journal of Geophysical Research*, *88*(A11), 8959–8970. https://doi.org/10.1029/JA088iA11p08959

Le Contel, O., Leroy, P., Roux, A., Coillot, C., Alison, D., Bouabdellah, A., et al. (2016). The search-coil magnetometer for MMS. *Space Science Reviews*, *199*(1-4), 257–282. https://doi.org/10.1007/s11214-014-0096-9

Le Contel, O., Retinò, A., Breuillard, H., Mirioni, L., Robert, P., Chasapis, A., et al. (2016). Whistler mode waves and hall fields detected by MMS during a dayside magnetopause crossing. *Geophysical Research Letters*, *43*, 5943–5952. https://doi.org/10.1002/2016GL068968

Li, J., Bortnik, J., An, X., Li, W., Thorne, R. M., Zhou, M., et al. (2017). Chorus wave modulation of Langmuir waves in the radiation belts. *Geophysical Research Letters*, *44*, 11,713–11,721. https://doi.org/10.1002/2017GL075877

Li, W., Thorne, R. M., Bortnik, J., Shprits, Y. Y., Nishimura, Y., Angelopoulos, V., et al. (2011). Typical properties of rising and falling tone chorus waves. *Geophysical Research Letters*, *38*, L14103. https://doi.org/10.1029/2011GL047925

Li, W., Thorne, R. M., Nishimura, Y., Bortnik, J., Angelopoulos, V., McFadden, J. P., et al. (2010). THEMIS analysis of observed equatorial electron distributions responsible for the chorus excitation. *J. Geophys. Res.*, *115*, A00F11. https://doi.org/10.1029/2009JA014845

Lindqvist, P.-A., Olsson, G., Torbert, R. B., King, B., Granoff, M., Rau, D., et al. (2016). The spin-plane double probe electric field instrument for MMS. *Space Science Reviews*, *199*(1-4), 137–165. https://doi.org/10.1007/s11214-014-0116-9

Mandt, M. E., Denton, R. E., & Drake, J. F. (1994). Transition to whistler mediated magnetic reconnection. *Geophysical Research Letters*, *21*(1), 73–76. https://doi.org/10.1029/93GL03382

Means, J. D. (1972). Use of the three-dimensional covariance matrix in analyzing the polarization properties of plane waves. *Journal of Geophysical Research*, *77*(28), 5551–5559. https://doi.org/10.1029/JA077i028p05551

Mourenas, D., Artemyev, A. V., Agapitov, O. V., Krasnoselskikh, V., & Mozer, F. S. (2015). Very oblique whistler generation by low-energy electron streams. *Journal of Geophysical Research: Space Physics*, *120*, 3665–3683. https://doi.org/10.1002/2015JA021135

Nunn, D., & Omura, Y. (2015). A computational and theoretical investigation of nonlinear wave-particle interactions in oblique whistlers. *Journal of Geophysical Research: Space Physics*, *120*, 2890–2911. https://doi.org/10.1002/2014JA020898

Omura, Y., & Summers, D. (2006). Dynamics of high-energy electrons interacting with whistler mode chorus emissions in the magnetosphere. *Journal of Geophysical Research*, *111*, A09222. https://doi.org/10.1029/2006JA011600

Pollock, C. J., Moore, T., Jacques, A., Burch, J., Gliese, U., Saito, Y., et al. (2016). Fast plasma investigation for magnetospheric multiscale. *Space Science Reviews*, *199*(1-4), 331–406. https://doi.org/10.1007/s11214-016-0245-4

Reinleitner, L. A., Gurnett, D. A., & Gallagher, D. L. (1982). Chorus-related electrostatic bursts in the Earth's outer magnetosphere. *Nature*, *295*(5844), 46–48. https://doi.org/10.1038/295046a0

Reinleitner, L. A., Gurnett, D. A., & Eastman, T. E. (1983). Electrostatic bursts generated by electrons in Landau Resonance with whistler mode chorus. *Journal of Geophysical Research*, *88*, 3079–3093.

Reinleitner, L. A., Kurth, W. S., & Gurnett, D. A. (1984). Chorus-related electrostatic bursts at Jupiter and Saturn. *Journal of Geophysical Research*, *89*(A1), 75–83. https://doi.org/10.1029/JA089iA01p00075

Russell, C. T., Anderson, B. J., Baumjohann, W., Bromund, K. R., Dearborn, D., Fischer, D., et al. (2016). The magnetospheric multiscale magnetometers. *Space Science Reviews*, *199*(1-4), 189–256. https://doi.org/10.1007/s11214-014-0057-3

Sharma, R. P., Pathak, N., Yadav, N., & Sharma, P. (2017). Nonlinear propagation of whistler wave and turbulent spectrum in reconnection region of magnetopause. *Physics of Plasmas*, *24*(9), 092902, https://doi.org/10.1063/1.4998475.

Shklyar, D., & Matsumoto, H. (2009). Oblique whistler-mode waves in the inhomogeneous magnetospheric plasma: Resonant interactions with energetic charged particles. *Surveys in Geophysics*, *30*(2), 55–104. https://doi.org/10.1007/s10712-009-9061-7

Shklyar, D. R. (2011). On the nature of particle energization via resonant wave-particle interaction in the inhomogeneous magnetospheric plasma. *Annales de Geophysique*, *29*(6), 1179–1188. https://doi.org/10.5194/angeo-29-1179-2011

Stix, T. H. (1962). *The theory of plasma waves*. New York: McGraw-Hill.

Tang, X., Cattell, C., Dombeck, J., Dai, L., Wilson, L. B. III, Breneman, A., & Hupach, A. (2013). THEMIS observations of the magnetopause electron diffusion region: Large amplitude waves and heated electrons. *Geophysical Research Letters*, *40*, 2884–2890. https://doi.org/10.1002/grl.50565

Torbert, R. B., Russell, C. T., Magnes, W., Ergun, R. E., Lindqvist, P. A., LeContel, O., et al. (2016). The FIELDS instrument suite on MMS: Scientific objectives, measurements, and data products. *Space Science Reviews*, *199*(1-4), 105–135. https://doi.org/10.1007/s11214-014-0109-8

Wilder, F. D., Ergun, R. E., Goodrich, K. A., Goldman, M. V., Newman, D. L., Malaspina, D. M., et al. (2016). Observations of whistler mode waves with nonlinear parallel electric fields near the dayside magnetic reconnection separatrix by the magnetospheric multiscale mission. *Geophysical Research Letters*, *43*, 5909–5917. https://doi.org/10.1002/2016GL069473

Wilder, F. D., Ergun, R. E., Newman, D. L., Goodrich, K. A., Trattner, K. J., Goldman, M. V., et al. (2017). The nonlinear behavior of whistler waves at the reconnecting dayside magnetopause as observed by the magnetospheric multiscale mission: A case study. *Journal of Geophysical Research: Space Physics*, *122*, 5487–5501. https://doi.org/10.1002/2017JA024062

Zhou, M., Ashour-Abdalla, M., Berchem, J., Walker, R. J., Liang, H., El-Alaoui, M., et al. (2016). Observation of high-frequency electrostatic waves in the vicinity of the reconnection ion region by the spacecraft of the magnetospheric multiscale (MMS) mission. *Geophysical Research Letters*, *43*, 4808–4815. https://doi.org/10.1002/2016GL069010

Zhou, M., Berchem, J., Walker, R. J., El-Alaoui, M., Goldstein, M. L., Lapenta, G., et al. (2018). Magnetospheric multiscale observations of an ion diffusion region with large guide field at the magnetopause: Current system, electron heating, and plasma waves. *Journal of Geophysical Research: Space Physics*, *123*, 1834–1852. https://doi.org/10.1002/2017JA024517